Chemical Science

EDGE ARTICLE

View Article Online
View Journal | View Issue



Cite this: *Chem. Sci.*, 2014, **5**, 707

# Transient electronic and vibrational absorption studies of the photo-Claisen and photo-Fries rearrangements†

Stephanie J. Harris,[a] Daniel Murdock,[a] Michael P. Grubb,[a] Gregory M. Greetham,[b] Ian P. Clark,[b] Michael Towrie[b] and Michael N. R. Ashfold*[a]

Received 18th October 2013
Accepted 21st November 2013

DOI: 10.1039/c3sc52893f

www.rsc.org/chemicalscience

The liquid-phase photo-Claisen and photo-Fries rearrangement dynamics of allyl phenyl ether and phenyl acetate in cyclohexane solution have been interrogated *via* ultrafast transient absorption spectroscopy. Following excitation at 267 nm, the reaction progress is monitored on a picosecond time-scale by electronic and vibrational absorption spectra obtained from broadband UV/Visible and mid-infrared probe pulses. The evolution of the ground and excited electronic states of the parent molecule, the radicals produced by photo-induced homolytic bond fission, and intermediate cyclohexadienones formed *via* recombination of the produced radical pair are followed, providing new insight and detail on the reaction mechanisms. Subsequent kinetic analysis allows determination of rate coefficients as well as quantum yields for the processes involved. These examples serve to highlight the utility of employing broadband UV-Visible and infrared probe spectroscopies, in conjunction, to unravel the mechanisms of photochemical reactions in solution. The underlying photo-physics that initiates bond fission in this class of molecules is also addressed in the context of the role of dissociative (n/π)σ* excited states.

## Introduction

The rearrangements of substituted phenols from either aryl phenyl ethers or phenyl esters into 2- or 4-substituted phenol products are a well-studied class of reactions in synthetic chemistry. First identified by Claisen[1] and Fries[2,3] in the early 1900's, the thermal Claisen rearrangement results in a 2-substituted phenol produced *via* a concerted intramolecular reaction whereas a Lewis acid catalyzes the Fries rearrangement and, depending on the experimental conditions, can result in either a 2- or a 4-substituted phenol. Several decades after these initial discoveries, photochemical versions of both rearrangements were uncovered, known as the photo-Claisen[4] and the photo-Fries rearrangements.[5,6] Subsequent mechanistic studies suggested that UV excitation of the reactant causes homolytic bond fission producing a radical pair which can then recombine to form the original parent molecule. Alternatively, the recombination can occur at either the 2- or 4-positions on the aromatic ring to form a cyclohexadienone intermediate which subsequently undergoes hydrogen atom transfer to form the corresponding substituted phenol as depicted in Scheme 1.[7–12] A previous ultrafast study of a 4-substituted phenyl acetate using a UV/Visible probe at several discrete wavelengths by Lochbrunner *et al.* provided time-resolved support of this mechanism.[13]

The thermal versions of these rearrangements have received extensive attention and evaluation as a key tool in a wide range of syntheses.[14–16] With improved understanding and further investigation, the photochemical versions of these rearrangements may offer the same synthetic utility as their thermal counterparts but with the added benefit of being a 'greener' synthetic route,[17] negating the need for additional reagents (in

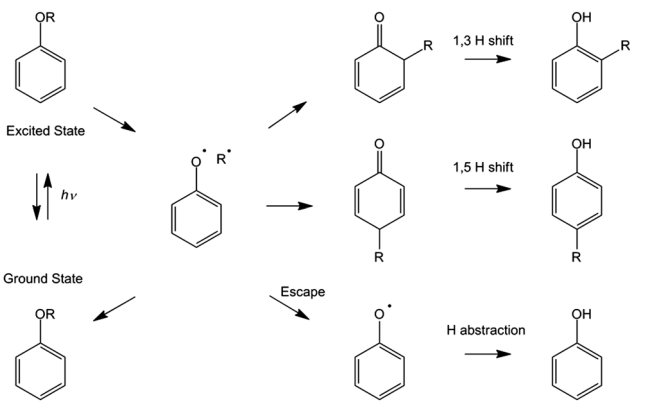


Scheme 1

[a]*School of Chemistry, University of Bristol, Bristol, BS8 1TS, UK. E-mail: mike.ashfold@bris.ac.uk*

[b]*Central Laser Facility, Research Complex at Harwell, Science and Technology Facilities Council, Rutherford Appleton Laboratory, Harwell Science and Innovation Campus, Didcot, Oxfordshire, OX11 0QX, UK*

† Electronic supplementary information (ESI) available. See DOI: 10.1039/c3sc52893f

the case of the Fries rearrangement) and, potentially, requiring reduced energy input. The photo-Fries reaction has previously been used synthetically for the production of compounds including diazoamide macrocycles,[18] hydroxyphenones[19] and chroman-4-one derivatives.[20] A photo-Fries rearrangement has also been identified as the main degradation process of paracetamol following UV excitation.[21] The photo-Claisen rearrangement has recently been used in micelle formation.[21]

This study uses both transient electronic absorption (TEA) and transient vibrational absorption (TVA) spectroscopy to follow the evolution of the species produced by the UV excitation of allyl phenyl ether ($PhOC_3H_5$) and phenyl acetate ($PhOC(O)CH_3$) in cyclohexane solution – well-known examples of the photo-Claisen and photo-Fries reactions. As we show below, the combination of transient interrogation by broadband UV/Visible and broadband IR probe pulses reveals a much fuller mechanistic picture of these photo-initiated rearrangements than either technique alone, allowing determination of production and loss rates for various key species and intermediates and estimates of quantum yields – information which, in turn, affords greater understanding of the underlying photophysics driving these processes.

## Experimental

The TEA and TVA spectra were recorded using the ULTRA laser facility at the STFC Rutherford Appleton Laboratory.[22] An amplified titanium sapphire laser system generated 800 nm (band center) pulses with 50 fs pulse duration at a 10 kHz repetition rate. The broadband UV/Visible probe was generated by focusing a portion of the 800 nm radiation into a $CaF_2$ disc which was rastered in the two planes orthogonal to beam propagation in order to reduce photodamage. A further portion of the 800 nm light was used to pump an optical parametric amplifier to produce mid-IR pulses with a bandwidth of $\sim$500 $cm^{-1}$. In each experiment the pump and probe pulses were overlapped in the sample with their respective linear polarization vectors aligned at the magic angle, before the transmitted radiation was dispersed by a grating onto a 512 element silicon array (for UV/Visible detection) or a 128 element mercury cadmium telluride array (for IR detection). The samples were flowed continuously through a Harrick cell with a 100 μm PTFE spacer between $CaF_2$ windows at solution concentrations chosen to ensure an absorbance of 0.5 at 267 nm (30 mM for $PhOC_3H_5$ and 180 mM for $PhOC(O)CH_3$). The $\sim$1 ps experimental response function is limited by background noise induced by the cell windows and solvent (cyclohexane), thus masking the true instrumental response time of $\sim$100 fs. $PhOC_3H_5$ (99%), $PhOC(O)CH_3$ (99%), and cyclohexane were obtained from Sigma-Aldrich and used without further purification.

## Results

### Transient absorption spectroscopy

We begin by considering the TEA spectra of $PhOC_3H_5$ and $PhOC(O)CH_3$ in cyclohexane shown in Fig. 1(a) and 2(a) respectively. At the earliest pump-probe delays studied, $\sim$2 ps, both systems exhibit a broad increase in absorption extending across the full probe region (340–670 nm). In accord with previous aromatic molecules studied *via* TEA these features can be assigned to absorption from an excited electronic state of the molecule under study.[23–25] The temporal evolution of these features are depicted in Fig. 1(c) and 2(d) and are fit well by a single exponential decay which provides a measure of the lifetime of the excited state molecule. A value of 96(4) ps (where the number in parentheses represents the one standard deviation uncertainty in the last significant digit) is obtained for $PhOC_3H_5$, while the data for $PhOC(O)CH_3$ reveal an excited state lifetime of 30(3) ps.

The TEA spectra of $PhOC_3H_5$ and $PhOC(O)CH_3$ exhibit another similarity, a structured feature at 398 nm. This feature has been observed several times previously and is assigned to the phenoxyl radical produced following O–R bond fission.[24–26] Due to the substantial overlap of this absorption with that of the excited state parent, the detailed kinetics of the phenoxyl radical cannot be obtained. Homolytic bond fission following UV excitation of $PhOC_3H_5$/$PhOC(O)CH_3$ will also produce an allyl/acetyl radical. No absorption of the allyl radical has been reported in the visible probe region studied here, but absorption due to the acetyl radical has previously been recorded in the 490–660 nm range ($\lambda_{max} = 532$ nm), with a measured absorption cross section, $\sigma = (1.1 \pm 0.2) \times 10^{-19}$ $cm^2$ per molecule (a molar extinction coefficient, $\varepsilon$, of 29 $M^{-1}$ $cm^{-1}$).[27] No feature attributable to the acetyl radical is evident at these wavelengths in Fig. 2(a), but this is not unexpected given the weakness of this absorption (*cf.* for phenoxyl at $\lambda_{max} = 398$ nm, $\sigma = 1.2 \times 10^{-17}$ $cm^2$ per molecule, $\varepsilon = 3155$ $M^{-1}$ $cm^{-1}$).[26]

The TVA spectra recorded following 267 nm photoexcitation of $PhOC_3H_5$ and $PhOC(O)CH_3$ are shown in Fig. 1(b), 2(b) and (c), respectively. The spectra of $PhOC_3H_5$ show six features within the probe region studied (1400–1700 $cm^{-1}$), three bleach features reflecting depletion of the ground state population induced by the UV pump pulse at 1495, 1586 and 1598 $cm^{-1}$ (with strong overlap been the latter two features) and three transient absorptions at 1415, 1516 and 1672 $cm^{-1}$.

As shown by the kinetic traces in Fig. 1(c) and (d), the transient absorption features at 1415 and 1516 $cm^{-1}$ show very different kinetic behavior from that exhibited by the feature centered at 1672 $cm^{-1}$. Fig. 1(c) shows the transient behavior of the feature at 1415 $cm^{-1}$. It exhibits an exponential decay with a time constant of 108(8) ps. This transient population change suggests that the feature can be assigned to absorption of the excited state of $PhOC_3H_5$ as its lifetime is comparable to that of the excited state absorption (ESA) recorded in the TEA spectra; when these two kinetic traces are fit simultaneously to an exponential decay a lifetime of 98(4) ps is obtained. The other transient absorption at 1672 $cm^{-1}$ shows different kinetics; it is first visible at pump-probe delays of $\sim$10 ps and grows with an exponential rise time of 150(10) ps. Given this kinetic evolution, it might initially appear tempting to assign this feature to absorption of the phenoxyl radical previously identified in the TEA spectra. This assignment would be incorrect, however, as both previous measurements and calculations do not find or

 

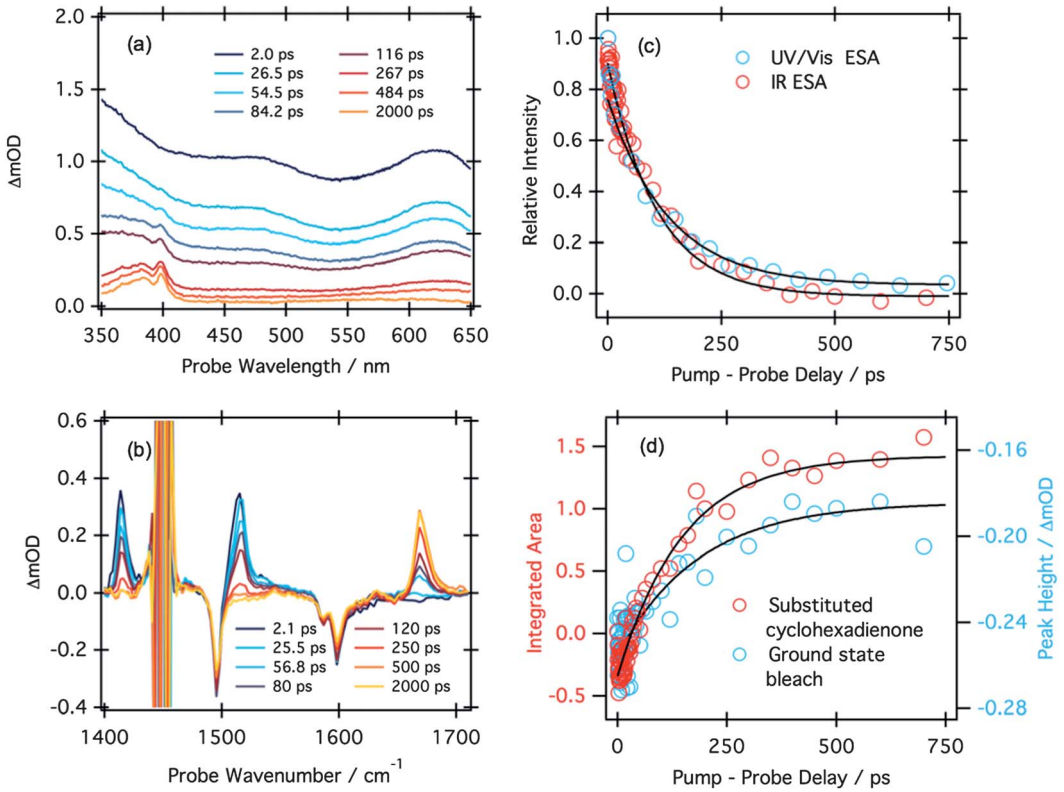


Fig. 1 Representative transient absorption spectra of a solution of $PhOC_3H_5$ (30 mM in cyclohexane) following excitation at 267 nm and probing (a) in the UV/Visible region (350–650 nm) and (b) in the mid-IR between 1400 $cm^{-1}$ and 1710 $cm^{-1}$ at various pump – probe delays (the feature at 1450 $cm^{-1}$ arises as a result of absorption by the cyclohexane solvent). (c) Traces showing the normalized intensity of ESA in both the TEA (taken at 485 nm, blue) and TVA (integrated intensity of the 1415 $cm^{-1}$ band, red) experiments as a function of time. (d) The time evolution of the integrated areas of the 1672 $cm^{-1}$ band attributed to the cyclohexadienone intermediate (red) and of the ground state bleach recovery (blue) of the 1598 $cm^{-1}$ band. The solid lines in (c) and (d) are the kinetic fits to the data as described in the text.

predict any phenoxyl radical absorption in the 1670 $cm^{-1}$ region.[28] Instead, absorptions in this mid-IR wavenumber region are usually associated with a carbonyl group. Two of the proposed intermediates contain a carbonyl group, *viz.* the substituted 2,4- and 2,5-cyclohexadienones. These are formed when the produced radical pair geminately recombines with, in this case, the aliphatic group rejoining the phenoxyl at either the 2 or the 4 position. However, the predicted carbonyl stretching wavenumbers for these two species are very similar and cannot be distinguished in this experiment (Tables 1 and 2 in the ESI† detail the calculations of the normal modes of $PhOC_3H_5$, $PhOC(O)CH_3$ and the substituted 2,4- and 2,5-cyclohexadienone intermediates that have aided these assignments).

Fig. 2(b) and (c) show the TVA spectra obtained for $PhOC(O)CH_3$ with a probe range of 1530–1850 $cm^{-1}$ and 1810–2000 $cm^{-1}$, respectively. In this range and over all time delays eight features are discernible, two bleach features at 1604 and 1820 $cm^{-1}$ and six transient absorption features at 1546, 1557, 1697, 1765, 1803 and 1864 $cm^{-1}$. Again, the bleaches reflect depopulation of the $S_0$ state of $PhOC(O)CH_3$ by the UV pump pulse. Two of the six transient absorption features, at 1557 and 1803 $cm^{-1}$, are evident at the earliest pump – probe delays and decay exponentially with a time constant of 28(1) ps. Comparison of this decay constant with those obtained from the analysis of TEA data suggests that these two features correspond to excited state absorption. The same lifetime (28(1) ps) is obtained when the kinetic traces obtained from the TEA and TVA experiments are fit simultaneously.

The feature at 1866 $cm^{-1}$ exhibits distinctly different kinetic behaviour from the other transient features and is shown in Fig. 2(e). The feature grows for ~40 ps following excitation, and then begins to decay with some fraction remaining at long time delays. This kinetic behaviour, and the wavenumber at which the band appears, suggests that the feature is due to the acetyl radical produced *via* O–R bond fission. Previous measurements of the IR spectrum of the acetyl radical in hexane solutions, which found a C=O stretching wavenumber of 1864 $cm^{-1}$, serve to reinforce this assignment.[29] Its appearance reflects production by bond fission from the initially excited electronic state of the parent molecule, whereas its subsequent decay is attributable to geminate recombination to form the aforementioned substituted cyclohexadienones or the $S_0$ state parent molecule. The long-time absorption indicates that some fraction of the radical products escapes recombination and persists beyond 2.5 ns in solution.

The two features at 1697 and 1765 $cm^{-1}$ evolve concurrently and, analogous to $PhOC_3H_5$, can be ascribed to formation of either or both the substituted 2,5- or 2,4-cyclohexadienone

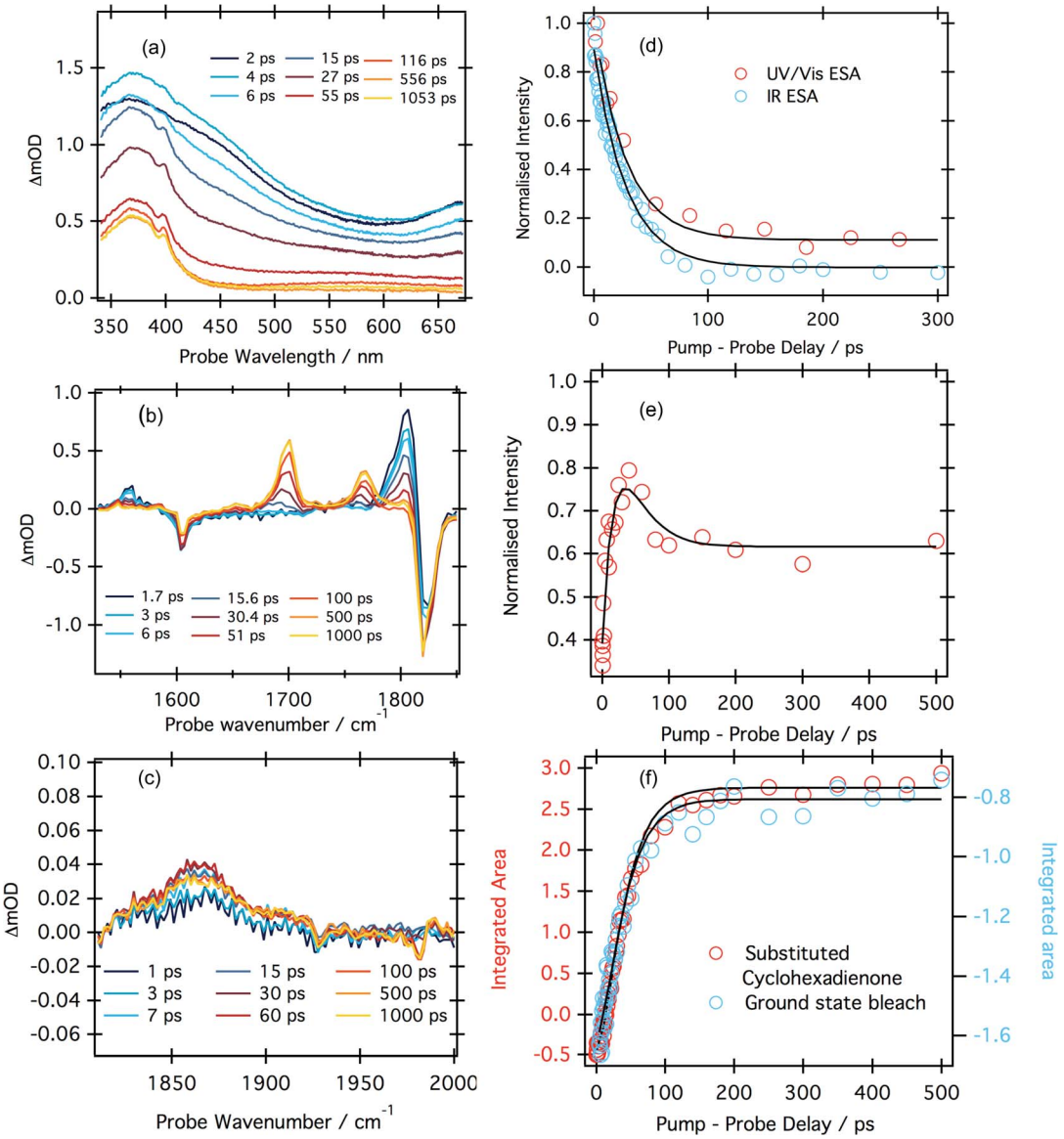


Fig. 2 Representative transient absorption spectra of a solution of $PhOC(O)CH_3$ (180 mM in cyclohexane) following excitation at 267 nm and probing (a) the UV/Visible region (340–670 nm) (b) in the mid-IR between 1530 $cm^{-1}$ and 1850 $cm^{-1}$ and (c) in the mid-IR from 1810–2000 $cm^{-1}$ at various pump – probe delays. (d) Traces showing the transient behavior of the ESA observed both in the TEA (at a single wavelength of 524 nm) and in the TVA (at 1807 $cm^{-1}$) experiments and (e) the transient evolution of the integrated area of the 1864 $cm^{-1}$ acetyl radical band. (f) Traces indicating the time evolution of the feature assigned to the substituted adduct (1678–1717 $cm^{-1}$, red) and the ground state bleach recovery (blue). The solid lines in (d)–(f) are the kinetic fits to the data as described in the text.

intermediates. The intermediates in this case show two C=O stretch absorptions, as two distinct carbonyl groups are present: the enone, which is part of the six-membered ring (at 1697 $cm^{-1}$) and the carbonyl of the acetyl group (at 1765 $cm^{-1}$). These features exhibit an exponential rise of 48(2) ps. As was the case for $PhOC_3H_5$, the predicted wavenumbers of the carbonyl stretching modes in the substituted cyclohexadienones are too close to allow them to be differentiated in the present TVA spectra. However, the predicted IR transition strengths (detailed in the ESI†) offer another possible route to discriminating between these two intermediates. The calculated ratio of the enone to acetyl C=O stretch band intensities is 0.98 in the case of the 2-substituted cyclohexadienone, while in the 4-substituted cyclohexadienone it is 2.3. The experimentally observed ratio is 1.9. If the calculated IR intensities are reliable, this would suggest that the ratio of substituted 2,5-cyclohexadienone to 2,4-cyclohexadienone is ~2 : 1. The previous time resolved study of the photo-Fries rearrangement used a 4-substituted phenyl acetate specifically to exclude possible competition between the two sites of cyclohexadienone formation.[13]

The TVA spectra also allow any repopulation of the ground electronic state of these two molecules to be monitored *via* the intensity of the ground state bleach features. Fig. 1(d) and 2(f) show that, over the timescale probed, 2.5 ns, ~30% of the initially excited population of $PhOC_3H_5$ returns to the $S_0$ state

 

while, for $PhOC(O)CH_3$, this recovery is ~54%. When the extracted kinetic traces are fit to an exponential function, good agreement with the rise time for formation of the intermediate cyclohexadienones (170(35) ps and 60(10) ps for $PhOC_3H_5$ and $PhOC(O)CH_3$, respectively) is found. We recognize that internal conversion (IC) from the photoexcited state could contribute to the parent bleach recovery at early pump-probe delays, but any such contribution is hard to discern in the present data as the excited state lifetimes in both systems are similar to that observed for geminate recombination. Any contribution from IC is thus neglected in the following kinetic analysis.

### Kinetic modelling

Scheme 2 details the kinetic scheme used to model the processes observed in the photo-Claisen and photo-Fries rearrangements of $PhOC_3H_5$ and $PhOC(O)CH_3$, respectively. $k_d$ is the rate coefficient for dissociation of the photo-excited molecule to form a radical pair, $PhO^{\cdot}$ + $R^{\cdot}$. This radical pair can then be lost in two ways; recombination (described by a rate coefficient $k_r$) or escape into the bulk solvent, yielding $PhO^{\cdot}_e$ + $R^{\cdot}_e$ (described by the rate coefficient $k_e$). Recombination can lead to several observable products: $S_0$ parent molecules and the substituted 2,4- and 2,5-cyclohexadienones. An analogous scheme has been used previously to model the kinetics of electron photodetachment from halide anions.[30,31]

Treating the ($PhO^{\cdot}$ + $R^{\cdot}$) radical pair as a single entity allows analytical solutions for the time dependent concentrations of the four species of interest to be obtained. This treatment has been favoured over one where the geminate recombination process is modelled diffusionally,[31] with the assumption that the radical pair is formed instantaneously after UV excitation. Since the lifetimes of the electronically excited parent molecules are in the tens of ps range, such an assumption would be inappropriate in this case. In the case of $PhOC(O)CH_3$, all the transient populations necessary for complete kinetic modelling (*viz.* the excited and ground electronic states of the parent molecule, the substituted cyclohexadiene, and the $C(O)CH_3$ radical) are accessible. It is important to note that the "in cage" and "bulk" acetyl radicals have the same spectral signature, and the observed signal is consequently the sum of both. Fitting all of the available data, simultaneously, to the kinetic equations detailed in the ESI† yields the rate coefficients and quantum yields shown in Table 1.

In deriving the latter, we assume an initial quantum yield for dissociation, $\phi_d = 1$. $\phi_r$ and $\phi_e$ are the respective quantum yields for recombination and escape which can be obtained from the relative magnitudes of $k_e$ and $k_r$. The quantum yield for recombination is itself the sum of that for reforming $S_0$ parent molecules, $\phi_{S0}$, and that for forming the cyclohexadienone adducts, $\phi_{CHD}$. The percentage ground state bleach recovery provides a measure of $\phi_{S0}$, with $\phi_{CHD}$ subsequently being obtained from the relation $\phi_r = \phi_{S0} + \phi_{CHD}$.

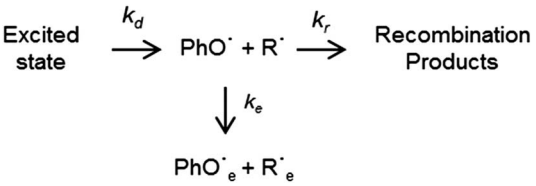


Scheme 2

Table 1 Rate coefficients and quantum yields determined for the processes involved in the photo-initiated rearrangements of $PhOC(O)CH_3$ and $PhOC_3H_5$[a]

| | $PhOC(O)CH_3$ | $PhOC_3H_5$ |
|---|---|---|
| $k_d$ | 0.0356(8) $ps^{-1}$ | 0.0102(4) $ps^{-1}$ |
| $k_r$ | 0.034(3) $ps^{-1}$ | — |
| $k_e$ | 0.012(1) $ps^{-1}$ | — |
| $\phi_r$ | 0.74(8) | 0.86 |
| $\phi_{S0}$ | 0.54 | 0.30 |
| $\phi_{CHD}$ | 0.20 | 0.56 |
| $\phi_e$ | 0.26(8) | 0.14 |

[a] The values with errors in parentheses are obtained or derived from the described kinetic modelling whilst the other quantum yields are estimated from these values.

Equivalent kinetic analysis for $PhOC_3H_5$ is hampered by the lack of transient signal for the $C_3H_5$ radical. $k_d$ has been acquired from analysis of the transient excited state population, but reliable values for $k_r$ and $k_e$ are unobtainable. The TEA experiments do, however, provide a relative measure of the long-time phenoxyl radical product yield for both molecules. The above analysis for $PhOC(O)CH_3$ shows that the long-time phenoxyl radical yield ($PhO^{\cdot}_e$) represents 26% of the originally excited population. Direct comparison of the relative intensities of the long-time phenoxyl absorption at 398 nm thus provides the estimate $\phi_e = 0.14$ in the case of $PhOC_3H_5$. Such a comparison is valid as the initial sample concentrations were chosen to ensure the same optical density, 0.5, at the excitation wavelength of 267 nm. Recalling Scheme 2, $\phi_e = 0.14$ implies that the total recombination quantum yield following 267 nm excitation of $PhOC_3H_5$ is $\phi_r = 0.86$. As for $PhOC(O)CH_3$, $\phi_{S0}$ can be obtained from analysis of the ground state bleach recovery, yielding $\phi_{S0} = 0.30$ and thus, by difference, $\phi_{CHD} = 0.56$.

## Discussion

The combined use of TEA and TVA techniques has allowed direct confirmation of the mechanism for the first few steps of the photo-Claisen and photo-Fries reactions shown in Scheme 1, while kinetic modeling has provided additional information about the timescales on which these processes occur and their respective quantum yields. Both techniques reveal absorption attributable to the respective excited state molecules and give dissociation lifetimes (in cyclohexane) of 96(4) ps for $PhOC_3H_5$ and 28(1) ps for $PhOC(O)CH_3$. Homolytic O–R bond fission is identified as the main population loss channel following photoexcitation. IC to the $S_0$ state cannot be completely ruled out, but is considered a minor process on the basis that the ground state bleach recovery exhibits the same early time kinetics to that of a process (adduct formation) that is unquestionably due to geminate recombination.

The tens of picoseconds excited state lifetimes identified in the present study provide a measure of the rate at which population transfers from the initial excited state to one of a dissociative nature. The excited state potential energy landscape relevant to O–R bond fission in a range of aromatic compounds, including $PhOC_3H_5$ and $PhOC(O)CH_3$, was explored in an early theoretical paper.[32] This study found the $S_1$ state of $PhOC_3H_5$ to be a $^1\pi\pi^*$ state, the PES of which is intersected by a dissociative $^1\pi\sigma^*$ state (where the $\sigma^*$ orbital is located along the O–R bond) correlating to PhO + $C_3H_5$ products. The acetyl group in $PhOC(O)CH_3$ introduces additional non-bonding and weakly antibonding orbitals. The $S_1$ state in this case was shown to have substantial carbonyl-centered $^1n\pi^*$ character (*i.e.* to be formed by removing an electron from an n-orbital on the carbonyl O atom to the $\pi^*$ orbital of the acetyl group), $S_2$ is the ring-centered $^1\pi\pi^*$ state and $S_3$ is the dissociative $^1\pi\sigma^*$ state that forms conical intersections (CIs) with both the $^1n\pi^*$ and $^1\pi\pi^*$ states at short $R_{O-R}$ bond lengths and with the $S_0$ state at longer $R_{O-R}$. The $^1n\pi^*$ and $^1\pi\pi^*$ states were predicted to lie close in energy, however, and it is not clear which excited state contributes most of the oscillator strength when exciting at 267 nm. These early calculations[32] also imply the existence of a barrier to O–R bond dissociation from the $S_1$ potential minimum ($PhOC_3H_5$) or from that of the $S_2$ state ($PhOC(O)CH_3$).

Given that UV excitation of both $PhOC_3H_5$ and $PhOC(O)CH_3$ results in homolytic O–R bond fission and formation of a radical pair that includes a phenoxyl radical, the well-studied case of phenol (PhOH) is an appropriate point from which to attempt to rationalise the photophysics of $PhOC_3H_5$ and $PhOC(O)CH_3$. The potential energy landscape of phenol is qualitatively similar to those exhibited by $PhOC_3H_5$ and $PhOC(O)CH_3$. O–H bond fission is observed even when exciting to $S_1(^1\pi\pi^*)$ levels lying at energies below the $S_1(^1\pi\pi^*)/S_2(^1\pi\sigma^*)$ CI, *i.e.* where there is a significant energy barrier to dissociation.[33] Time-resolved measurements show the H atom yield rising on a nanosecond timescale,[34] which can be understood in terms of O–H bond dissociation by tunneling through the barrier under the $S_1/S_2$ CI. At shorter excitation wavelengths (*i.e.* at energies above the $S_1/S_2$ CI), O–H bond fission occurs on a much faster timescale – either as a result of directly populating the dissociative $S_2$ state or following fast radiationless transfer to the $S_2$ PES following initial population of the higher lying $S_3(^1\pi\pi^*)$ state.[35] One key difference between the PESs of $PhOC_3H_5$, $PhOC(O)CH_3$ and phenol is the difference in bond dissociation energies (*i.e.* the asymptotic energy associated with radical production). The PhO–H bond strength in phenol is 3.72 eV whereas the PhO–R bond strengths in $PhOC_3H_5$ and $PhOC(O)CH_3$ are only 2.16 eV and 3.35 eV, respectively.[36] These reduced bond strengths reflect the additional stability of the allyl and acetyl radicals relative to the hydrogen atom produced by phenol photolysis. Recent pump-probe TEA experiments confirm that the same photoexcitation and dissociation dynamics persist for phenol in solution in weakly interacting solvents like cyclohexane though, unsurprisingly, additional post-excitation processes such as geminate recombination of the PhO + H products are also observed.[24,25]

How then can we reconcile excited state dissociation on a ps timescale following excitation of $PhOC_3H_5$ and $PhOC(O)CH_3$? Several points merit note. The topologies of the excited state PESs for $PhOC_3H_5$ and $PhOC(O)CH_3$ may be qualitatively similar to that of phenol, but the fragments formed *via* homolytic O–R bond fission are very different; allyl and acetyl are much larger than an H atom, and tunneling is not a credible fragmentation mechanism. A second consideration is the nature of the level or levels within the excited state manifold that will be populated by absorption of a 267 nm photon. The $S_1$–$S_0$ origin of $PhOC_3H_5$ in the gas phase has been identified at 4.50 eV, so absorption of a 267 nm photon (with energy 4.67 eV) will not form $PhOC_3H_5(S_1)$ molecules with substantial internal (vibrational) excitation. Indeed, given that the systems under study are solvated, any such vibrational energy is likely to be quenched by vibrational energy transfer to the surrounding solvent bath. Vibrational cooling in similar systems has been seen to occur on timescales of ~10 ps (ref. 37) and should thus be competitive for systems such as $PhOC_3H_5$ and $PhOC(O)CH_3$ with deduced $S_1$ lifetimes of tens of picoseconds.

Nonetheless, the present data confirm O–R bond fission to be the dominant decay process following 267 nm photoexcitation of both $PhOC_3H_5$ and $PhOC(O)CH_3$ as did the previous study of a 4-substituted phenyl acetate,[13] and it is pertinent to consider possible limitations of the previous theoretical treatment. The cuts along $R_{O-R}$ in these early PES calculations[32] were constrained to $C_s$ geometries (*i.e.* all the heavy atoms were held in a plane), but a later combined experimental (laser induced fluorescence) and theoretical study of isolated $PhOC_3H_5$ identified no fewer than four conformers lying within 500 $cm^{-1}$ of the planar ground state minimum.[38] Recent studies of S–$CH_3$ bond fission in thioanisoles may also be relevant in this regard. As in the phenols, the CI between the bound $S_1(^1\pi\pi^*)$ and dissociative $S_2(^1\pi\sigma^*)$ states of thioanisole is calculated to lie at energies above that of the $S_1(v = 0)$ level at planar geometries,[39] but the barrier to dissociation is seen to decrease upon relaxing the excited state geometry and by changing the C–S–$CH_3$ torsion angle.[40] For completeness, we note that the early theoretical study of $PhOC(O)CH_3$ did explore the effect of varying the torsion angle, but found no decrease in the height of the barrier to O–R bond fission.[32] New multi-dimensional *ab initio* calculations on these systems would surely be useful in helping to reconcile the present (and related)[13] experimental data. Of course, solvation could also contribute to this apparent mismatch between experiment and theory. Inspection of the available absorption data, presented in the ESI,† shows some red-shift in the peak of the long wavelength UV absorption spectrum of $PhOC_3H_5$ in cyclohexane (*cf.* the gas phase), but the real quantity of interest would be any differential shift in the relative energies of the bound $^1\pi\pi^*(^1n\pi^*)$ states and the dissociative $^1\pi\sigma^*$ PES (since this would affect the height of any barrier under this CI). The low oscillator strength and the diffuseness of the $\sigma^* \leftarrow \pi$ transition precludes its direct observation in absorption measurements.

Post-dissociation, the next step in Scheme 1 determines the fate of the radical pair. This involves competition between two processes: geminate recombination and solvent cage escape.

 

The former leads either to reforming the parent precursor or formation of a substituted cyclohexadienone. As noted above, this substitution may occur at either the 2- or 4-position on the ring (defined relative to the C–O bond) but neither of the present probe techniques allows us to distinguish between these two intermediates. Cage escape leads to a persistent radical signal. In the case of $PhOC(O)CH_3$, the present kinetic modeling suggests that the recombination rate in cyclohexane is ~3-times faster than the rate of radical cage escape; for $PhOC_3H_5$, the relative probability of radical pair recombination is yet greater (~86%). A more striking difference between the two systems is the relative branching among the recombination products. For $PhOC_3H_5$, about two thirds of the recombination events result in substituted cyclohexadienones whereas, for $PhOC(O)CH_3$, the majority recombination product is the $S_0$ parent molecule. A plausible explanation for this difference is that once on the $^1\pi\sigma^*$ PES, the separating $PhO\cdots C_3H_5$ products are well posed to recombine in a manner analogous to the concerted reaction observed in the thermal Claisen rearrangement. Such a mechanism should result in preferential production of the substituted 2,4-cyclohexadienone. No such pathway exists for the Fries rearrangement of $PhOC(O)CH_3$, consistent with the deduced lower fractional branching into the adduct in this case.

The final step in Scheme 1 is intramolecular hydrogen transfer within the cyclohexadienone intermediate to form the final substituted phenol product. The present TVA experiments are also capable of probing in the 3000 $cm^{-1}$ spectral region, where the O–H stretch vibration associated with creation of a phenol product should appear, but no such signal was observed even at the longest pump-probe delays (2.5 ns) – consistent with previous experimental estimates of the timescale on which hydrogen atom transfer occurs in these systems.[7,10,13]

## Conclusions

By using a combination of transient electronic and vibrational absorption spectroscopies, the temporal evolution of the photo-Claisen and photo-Fries rearrangements of $PhOC_3H_5$ and $PhOC(O)CH_3$ in cyclohexane solution have been followed for several nanoseconds following photoexcitation at 267 nm. During this time window, the ability to follow both electronic and vibrational absorption of the samples has allowed us to monitor the evolving population of the photoexcited parent molecule and the ensuing O–R bond fission (revealed by the appearance of phenoxyl radical absorption in the TEA experiment and, in the case of $PhOC(O)CH_3$, absorption due to the acetyl radical in the TVA experiment). Subsequent geminate recombination of the resulting radical pair – either to yield a substituted cyclohexadienone intermediate or to reform the parent molecule – is observed also, *via* growth of new absorption features and ground state bleach recovery in the TVA experiment. The final step in both the photo-Claisen and photo-Fries rearrangements, involving intramolecular hydrogen transfer to transform the cyclohexadienone intermediate into a substituted phenol, is not observed within the time delays probed.

Kinetic modelling of the time evolving signals of the various observed species has allowed determination of rate coefficients for each of the above processes, and their relative quantum yields. The fraction of radical pairs formed following photoexcitation that are deduced to escape the initial solvent cage is greater for $PhOC(O)CH_3$ (~26%) than for $PhOC_3H_5$ (14%). Thus most of the radical pairs formed in both cases undergo geminate recombination – but with different outcomes. In the case of $PhOC(O)CH_3$, reforming parent $S_0$ population is favoured over formation of the substituted cyclohexadienone intermediate by a factor of ~2 : 1, whereas $PhOC_3H_5$ shows the opposite behavior. This, we suggest, reflects the fact that the nascent allyl radical arising upon O–R bond fission in the latter case is particularly well posed to add at the 2-position of the ring (as in the thermal Claisen rearrangement).

At a more general level, the present study provides further illustrations of (i) the similarities between the primary UV photochemistry that drives O–R bond fission in these molecules and that responsible for O–H bond fission in simpler systems like phenol, (ii) the ubiquity of $\pi\sigma^*$ excited states in driving excited state bond fissions in such molecules, and (iii) the utility of detailed gas phase studies of simpler prototypes in guiding our understanding of the, usually more complex, photochemistry of condensed-phase systems for which little gas-phase spectroscopy is available and/or for which high-level theoretical calculations are prohibitive (due to the size of the molecules involved). The present study also highlights the value of broadband transient absorption methods (over the widest possible range of probe wavelengths)[41] for elucidating mechanistic aspects of photo-initiated organic reactions in solution – allowing identification of key species, the timescales on which they are created or destroyed and the respective product yields.

## Notes and references

1 L. Claisen, *Chem. Ber.*, 1912, **45**, 3175.
2 K. Fries and G. Finck, *Chem. Ber.*, 1908, **41**, 4271–4284.
3 K. Fries and W. Pfaffendorf, *Chem. Ber.*, 1910, **43**, 212–219.
4 M. S. Kharesch, G. Stampa and W. Nudenberg, *Science*, 1952, **116**, 309.
5 J. C. Anderson and C. B. Reese, *Proc. Chem. Soc.*, 1960, 217.
6 J. C. Anderson and C. B. Reese, *J. Chem. Soc.*, 1963, 1781–1784.
7 E. Kalmus and D. M. Hercules, *J. Am. Chem. Soc.*, 1972, **96**, 449–456.
8 S. M. Beck and L. E. Brus, *J. Am. Chem. Soc.*, 1982, **104**, 1805–1808.
9 A. L. Pincock, J. A. Pincock and R. Stefanova, *J. Am. Chem. Soc.*, 2002, **124**, 9768–9778.
10 F. Galindo, *J. Photochem. Photobiol., C*, 2005, **6**, 123–138.
11 I. Iwakura, *Phys. Chem. Chem. Phys.*, 2011, **13**, 5546–5555.
12 I. Iwakura, A. Yabushita, J. Liu, K. Okamura and T. Kobayashi, *Phys. Chem. Chem. Phys.*, 2012, **14**, 9696–9701.
13 S. Lochbrunner, M. Zissler, J. Piel, E. Riedle, A. Spiegel and T. Bach, *J. Chem. Phys.*, 2004, **120**, 11634–11639.
14 F. E. Ziegler, *Chem. Rev.*, 1988, **88**, 1423–1452.
15 A. M. Martín Castro, *Chem. Rev.*, 2004, **104**, 2939–3002.

16 N. Hoffmann, *Chem. Rev.*, 2008, **108**, 1052–1103.
17 A. Albini and M. Fagnoni, *Green Chem.*, 2004, **6**, 1–6.
18 P. Magnus and C. Lescop, *Tetrahedron Lett.*, 2001, **42**, 7193–7196.
19 H. Kobsa, *J. Org. Chem.*, 1962, **27**, 2293–2298.
20 C. S. López, R. Erra-Balsells and S. M. Bonesi, *Tetrahedron Lett.*, 2010, **51**, 4387–4390.
21 M. Martignac, E. Oliveros, M.-T. Maurette, C. Claparols and F. Benoit-Marquié, *Photochem. Photobiol. Sci.*, 2013, **12**, 527–535.
22 G. M. Greetham, P. Burgos, Q. Cao, I. P. Clark, P. S. Codd, R. C. Farrow, M. W. George, P. Matousek, A. W. Parker, M. R. Pollard, A. Robinson, Z. Xin and M. Towrie, *Appl. Spectrosc.*, 2010, **64**, 1311–1319.
23 T. A. A. Oliver, Y. Zhang, M. N. R. Ashfold and S. E. Bradforth, *Faraday Discuss.*, 2011, **150**, 439–458.
24 Y. Zhang, T. A. A. Oliver, M. N. R. Ashfold and S. E. Bradforth, *Faraday Discuss.*, 2012, **157**, 141–163.
25 S. J. Harris, D. Murdock, Y. Zhang, T. A. A. Oliver, M. P. Grubb, A. J. Orr-Ewing, G. M. Greetham, I. P. Clark, M. Towrie, S. E. Bradforth and M. N. R. Ashfold, *Phys. Chem. Chem. Phys.*, 2013, **15**, 6567–6582.
26 X. Chen, D. S. Larsen, S. E. Bradforth and I. H. M. van Stokkum, *J. Phys. Chem. A*, 2011, **115**, 3807–3819.
27 B. Rajakumar, J. E. Flad, T. Gierczak, A. R. Ravishankara and J. B. Burkholder, *J. Phys. Chem. A*, 2007, **111**, 8950–8958.
28 B. M. Giuliano, I. Reva, L. Lapinski and R. Fausto, *J. Chem. Phys.*, 2012, **136**, 024505.
29 C. E. Brown, A. G. Neville, D. M. Rayner, K. U. Ingold and J. Lusztyk, *Aust. J. Chem.*, 1995, **48**, 363–379.
30 A. Staib and D. Borgis, *J. Chem. Phys.*, 1996, **104**, 9027.
31 J. A. Kloepfer, V. H. Vilchiz, V. A. Lenchenkov, A. C. Germaine and S. E. Bradforth, *J. Chem. Phys.*, 2000, **113**, 6288.
32 S. Grimme, *Chem. Phys.*, 1992, **163**, 313–330.
33 M. G. D. Nix, A. L. Devine, B. Cronin, R. N. Dixon and M. N. R. Ashfold, *J. Chem. Phys.*, 2006, **125**, 133318.
34 G. M. Roberts, A. S. Chatterley, J. D. Young and V. G. Stavros, *J. Phys. Chem. Lett.*, 2012, **3**, 348–352.
35 R. N. Dixon, T. A. A. Oliver and M. N. R. Ashfold, *J. Chem. Phys.*, 2011, **134**, 194303.
36 Y.-R. Lao, *Handbook of Bond Dissociation Energies in Organic Compounds*, 2003.
37 D. Murdock, S. J. Harris, T. N. V. Karsili, G. M. Greetham, I. P. Clark, M. Towrie, A. J. Orr-Ewing and M. N. R. Ashfold, *J. Phys. Chem. Lett.*, 2012, **3**, 3715–3720.
38 T. Isozaki, T. Suzuki and T. Ichimura, *Chem. Phys. Lett.*, 2007, **449**, 63–66.
39 J. S. Lim and S. K. Kim, *Nat. Chem.*, 2010, **2**, 627–632.
40 G. M. Roberts, D. J. Hadden, L. T. Bergendahl, A. M. Wenge, S. J. Harris, T. N. V. Karsili, M. N. R. Ashfold, M. J. Paterson and V. G. Stavros, *Chem. Sci.*, 2013, **4**, 993–1001.
41 E. Riedle, M. Bradler, M. Wenninger, C. F. Sailer and I. Pugliesi, *Faraday Discuss.*, 2013, **163**, 139.